Available online at www.sciencedirect.com
ScienceDirect
Journal of Computational Physics 220 (2006) 249–269
JOURNAL OF COMPUTATIONAL PHYSICS
www.elsevier.com/locate/jcp

High order finite difference methods for wave propagation in discontinuous media

Ken Mattsson [a,*], Jan Nordström [b,c]

[a] Center for Turbulence Research, Stanford University, Mechanical Engineering, Building 500, Room 500A, 488 Escondido Mall, Stanford, CA 94305-3035, United States
[b] Department of Information Technology, Scientific Computing, Uppsala University, P.O. Box 337, 75105 Uppsala, Sweden
[c] Department of Computational Physics, Division of System Technology, The Swedish Defense Research Agency, Stockholm, Sweden

Received 20 June 2005; received in revised form 8 February 2006; accepted 9 May 2006
Available online 30 June 2006

Abstract

High order finite difference approximations are derived for the second order wave equation with discontinuous coefficients, on rectangular geometries. The discontinuity is treated by splitting the domain at the discontinuities in a multi block fashion. Each sub-domain is discretized with compact second derivative summation by parts operators and the blocks are patched together to a global domain using the projection method. This guarantees a conservative, strictly stable and high order accurate scheme. The analysis is verified by numerical simulations in one and two spatial dimensions.

Keywords: High order finite difference methods; Wave equation; Numerical stability; Second derivatives; Discontinuous media

1. Introduction

For wave propagating problems, the computational domain is often large compared to the wavelengths, which means that waves have to travel long distances during long times. As a result, high order accurate time marching methods, as well as high order spatially accurate schemes (at least third order) are required. Such schemes, although they might be G-K-S stable [11] (convergence to the true solution as $\Delta x \to 0$),

* Corresponding author. Tel.: +1 650 723 0546; fax: +1 650 723 9617.
E-mail address: mattsson@stanford.edu (K. Mattsson).

0021-9991/$ - see front matter © 2006 Elsevier Inc. All rights reserved.
doi:10.1016/j.jcp.2006.05.007

may exhibit a non-physical growth in time [3], for realistic mesh sizes. It is therefore important to devise schemes that do not allow a growth in time that is not called for by the differential equation. Such schemes are called strictly (or time) stable.

In many applications, like general relativity [29], seismology and acoustics, the underlying equations are systems of second order hyperbolic partial differential equations. However (as pointed out in [15]), with very few exceptions, the equations are rewritten and solved on first order form. There are three obvious drawbacks with this approach, namely (i) we double the number of unknowns, (ii) we might introduce spurious oscillations (due to unresolved features), and (iii) we need twice as many grid points (both in time and in each of the spatial dimensions) to obtain the same accuracy. The reasons for solving the equations on first order form are probably due to the fact that computational methods for first order hyperbolic systems are very well developed, and they are naturally more suited for complex geometries.

For acoustic and electromagnetic wave propagation, staggered grid discretizations are very popular [6,31] since that avoids (ii) and (iii) above. Note however (again see [15]) that staggering in both time and space is more or less equivalent to solving the system of equations on second order form. One major disadvantage is that staggered grids do not have the summation by parts (SBP) property and that can lead to complications at boundaries and internal interfaces, especially for high order discretizations. To retain high order accuracy for problems with discontinuities in the coefficients is another concern [12,13,7].

The methods discussed above all solve the equations on first order form. Difference approximations have previously been derived [15,16,25,1,5] for the second order wave equation, without first writing it as a first order system. For problems with discontinuous coefficients at most second order accuracy have been recovered [1,5,13].

The second derivative terms have received little attention, especially concerning the stability issues for high order approximations [2]. Finite difference operators approximating second derivatives and satisfying a summation by parts rule, have previously been derived [20] for the 4th, 6th and 8th order case, with the emphasis on strictly stable formulations to mixed hyperbolic–parabolic problems.

One major advantage of using SBP operators [17,18,27] to discretize the equations on a multi block domain is that we can mimic the boundary and interface terms from the underlying continuous problem. Given the continuous boundary and interface conditions (i.e., the physics) in combination with the simultaneous approximation term (SAT) method [3,4,21,22] or the projection method [23,24] we can obtain completely analogous conservation and stability properties as for the underlying partial differential equation (PDE). This should attract physicists to employ this technique for a range of applications. In general relativity for example, the SBP operators combined with the SAT technique have now been successfully implemented [8,19] for system of equations on first order form (in time).

In this paper we will show how a certain class of the recently developed compact and high order accurate second derivative SBP operators [20] can be combined with the projection method for implementing general boundary and interface conditions. On piecewise rectangular domains we show that this technique leads to strictly stable and high order accurate schemes for the wave equation on second order form and discontinuous media. We will also show that the projection method requires special treatment at corners and block interfaces in two dimensions.

We focus on geometrically relative simple problems with piecewise constant coefficients and aim for high accuracy. Typical applications where this technique is appropriate include long range underwater acoustics (layers of air, water and soil), various seismological problems (layers of rock, water and possibly oil) as well as electromagnetic problems (wave guides and printed circuit boards). Complex geometries, varying coefficients and also the problem with absorbing boundary conditions [30,14] will not be addressed in this paper.

In Section 2 we introduce some definitions and discuss the SBP property for the second derivative. In Section 3 we consider the second order wave equation in one dimension (1-D) and show how the projection method and the SBP operators can be combined to obtain strictly stable schemes for problems with discontinuous coefficients. In Section 4 we consider the two-dimensional (2-D) problem. In Section 5 we describe a compact and explicit high order accurate time marching method that involves only two time levels. In Section 6, computations are done and in 7 conclusions are drawn. The SBP operators used in the computations are presented in Appendix II.

2. Definitions

To describe the SBP property in detail, some definitions are needed. The matrices and vectors

Name	Size	Non-zero elements
I_k	$(k+1,k+1)$	$(I_k)_{i,i}=1,\ i=0,k$
II_k	$(k-1,k+1)$	$(II_k)_{i,i+1}=1,\ i=0,k-2$
IL_k	$(k,k+1)$	$(IL_k)_{i,i+1}=1,\ i=0,k-1$
IR_k	$(k,k+1)$	$(IR_k)_{i,i}=1,\ i=0,k-1$
Il_k	$(1,k+1)$	$(Il_k)_0=1$
Ir_k	$(1,k+1)$	$(Il_k)_k=1$

(1)

will frequently be used in subsequent sections. We also need the notation

$$C\otimes D=\begin{bmatrix} c_{0,0}D & \cdots & c_{0,q-1}D \\ \vdots & & \vdots \\ c_{p-1,0}D & \cdots & c_{p-1,q-1}D \end{bmatrix},$$

where C is a $p\times q$ matrix and D a $m\times n$ matrix. The $p\times q$ block matrix $C\otimes D$ is called a *Kronecker product*. There are some useful rules for Kronecker products. In this paper we will use

$$\begin{aligned}&(A\otimes B)(C\otimes D)=(AC)\otimes(BD),\\ &(A\otimes B)^{\mathrm{T}}=A^{\mathrm{T}}\otimes B^{\mathrm{T}}.\end{aligned}\tag{2}$$

2.1. 1-D domains

Let the inner product for real valued functions $u,v\in\mathbf{L^2}[\mathbf{a},\mathbf{b}]$ be defined by $(u,v)=\int_a^b u^{\mathrm{T}}v\,\mathrm{d}x$, and let the corresponding norm be $\|u\|^2=(u,u)$. We also introduce a weighted norm

$$\|u\|_\omega^2=\int_a^b u^{\mathrm{T}}u\omega(x)\,\mathrm{d}x,$$

where $\omega(x)\in\mathbf{L^2}[\mathbf{a},\mathbf{b}]$ is a positive function. The domain $(a\leqslant x\leqslant b)$ is discretized using $N+1$ equidistant grid points,

$$x_i=a+\mathrm{i}h,\quad i=0,1,\ldots,N,\quad h=\frac{b-a}{N}.$$

The numerical approximation at grid point x_j is denoted v_j, and the discrete solution vector is $v^{\mathrm{T}}=[v_0,v_1,\ldots,v_N]$. We define an inner product for discrete real valued vector-functions $u,v\in\mathbf{R^{N+1}}$ by $(u,v)_H=u^{\mathrm{T}}Hv$, where $H=H^{\mathrm{T}}>0$, with a corresponding norm $\|v\|_H^2=v^{\mathrm{T}}Hv$.

2.2. 2-D domains

Consider the domain $(a\leqslant x\leqslant b,\ c\leqslant y\leqslant d)$ with an $N+1\times M+1$-points equidistant grid. That is,

$$\begin{aligned}&x_i=a+\mathrm{i}h_x,\quad i=0,1,\ldots,N,\quad h_x=\frac{b-a}{N},\\ &y_j=c+\mathrm{j}h_y,\quad j=0,1,\ldots,M,\quad h_y=\frac{c-d}{M}.\end{aligned}$$

The numerical approximation at grid point (x_i,y_j) is denoted $v_{i,j}$. We define a discrete solution vector $v^{\mathrm{T}}=[v^0,v^1,\ldots,v^N]$, where $v^k=[v_{k,0},v_{k,1},\ldots,v_{k,M}]$ is the solution vector at x_k along the y-direction, as illustrated in Fig. 1.

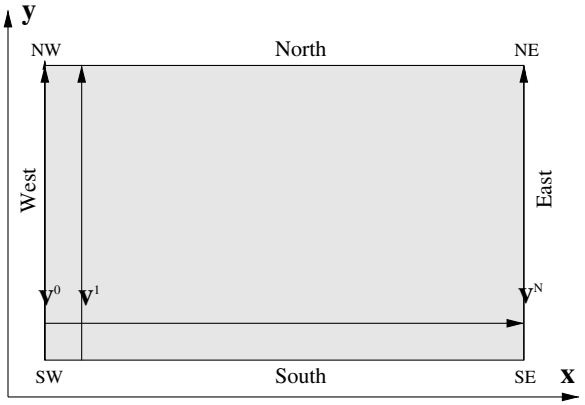

Fig. 1. Domain 2-D.

Let the inner product for real valued functions $u, v \in \mathbf{L^2}[\mathbf{x} \in [\mathbf{a}, \mathbf{b}],\ \mathbf{y} \in [\mathbf{c}, \mathbf{d}]]$ be defined by $(u, v) = \int_c^d \int_a^b u^{\mathrm{T}} v \,\mathrm{d}x \,\mathrm{d}y$, and let the corresponding norm be $\|u\|^2 = (u, u)$. We also introduce a weighted norm

$$\|u\|_\omega^2 = \int_c^d \int_a^b u^{\mathrm{T}} u \omega(x, y) \,\mathrm{d}x \,\mathrm{d}y,$$

where $\omega(x, y) \in \mathbf{L^2}[\mathbf{x} \in [\mathbf{a}, \mathbf{b}],\ \mathbf{y} \in [\mathbf{c}, \mathbf{d}]]$ is a positive function.

We define an inner product for discrete real valued vector-functions $u, v \in \mathbf{R^{N+1 \times M+1}}$ by $(u, v)_H = u^{\mathrm{T}} H v$, where $H = (H_x \otimes I_M)(I_N \otimes H_y) = H^{\mathrm{T}} > 0$, with a corresponding norm $\|v\|_H^2 = v^{\mathrm{T}} H v$. Here H_x and H_y denote the one-dimensional norms in the x- and y-direction, respectively. In order to distinguish (when necessary) if a difference operator P is working in the x or the y-directions we will use the notations P_x and P_y.

2.3. SBP property

An SBP operator mimic the behavior of the corresponding continuous operator with respect to the inner product mentioned above. High order accurate SBP operators for the first derivative has previously been developed [17,18] and refined [26]. To construct highly accurate and stable approximations of mixed hyperbolic–parabolic problems, high order accurate SBP operators for the *second* derivative were derived in [20], see also [4]. Before we discuss the SBP property for the second order wave equation it is instructive to first introduce the less restrictive SBP definition for parabolic problems. Consider the heat equation $u_t = u_{xx}$. Integration by parts (IBP) leads to

$$\frac{\mathrm{d}}{\mathrm{d}t}\|u\|^2 = (u, u_{xx}) + (u_{xx}, u) = 2u u_x|_a^b - 2\|u_x\|^2. \tag{3}$$

The construction (see [20]) of SBP operators D_2, approximating $\partial^2/\partial x^2$ were based on Eq. (3). To fully mimic the IBP property, we need $D_2 = H^{-1}(-D_1^{\mathrm{T}} H D_1 + BS)$, where D_1 is a consistent approximation of $\partial/\partial x$, S includes an approximation of the first derivative operator at the boundary, and $B = \mathrm{diag}(-1, 0, \ldots, 0, 1)$. By multiplying the semi-discrete approximation $v_t = D_2 v$ by $v^{\mathrm{T}} H$ and by adding the transpose, we obtain

$$\frac{\mathrm{d}}{\mathrm{d}t}\|v\|_H^2 = (v, D_2 v)_H + (D_2 v, v)_H = 2v_N (Sv)_N - 2v_0 (Sv)_0 - 2\|D_1 v\|_H^2. \tag{4}$$

Formula (4) is a discrete analog to the IBP formula (3) in the continuous case.

However, it is not necessary to fully mimic the IBP property to obtain an energy estimate for a parabolic problem. Consider the difference operator $H^{-1}(-A + BS)$, approximating $\partial^2/\partial x^2$. The energy method leads to

$$\frac{\mathrm{d}}{\mathrm{d}t}\|v\|_H^2 = 2v_N (Sv)_N - 2v_0 (Sv)_0 - v^{\mathrm{T}}(A + A^{\mathrm{T}})v. \tag{5}$$

To obtain an energy estimate it suffices that $A + A^{\mathrm{T}} \geqslant 0$, assuming that the boundary terms are correctly implemented.

In [20] we introduced the following definition.

Definition 2.1. A difference operator $D_2 = H^{-1}(-A + BS)$ approximating $\partial^2/\partial x^2$ is said to be a second derivative SBP operator if $A + A^{\mathrm{T}} \geqslant 0$, if S includes an approximation of the first derivative operator at the boundary and $B = \mathrm{diag}(-1, 0, \ldots, 0, 1)$.

However, as we will show in the following section, hyperbolic second order systems introduce an extra stability requirement (see Lemma 3.1 and Definition 3.2) on the SBP operator.

3. The projection method in 1-D

In this method developed by Olsson [23], the boundary conditions are introduced via an orthogonal projection. When the energy method is applied, the projection operator P interacts with the SBP operator to generate boundary terms that are completely analogous to those of the continuous problem. In this section we consider the one-dimensional problem. We will also discuss the extra stability requirement for the SBP operator, when applied to the wave equation on second order form.

3.1. Single domain

An energy estimate for the wave equation on second order form $u_{tt} = u_{xx} + F(x,t)$, $x \in [0,1]$ requires initial conditions $u(x,0) = f_1(x)$, $u_t(x,0) = f_2(x)$ and appropriate boundary conditions

$$L_l u = \alpha u(0,t) + u_x(0,t) = g_l(t), \quad L_r u = \beta u(1,t) + u_x(1,t) = g_r(t). \tag{6}$$

Remark. Other type of boundary conditions, like Dirichlet and radiation boundary conditions (see for example [30,14]) can also be used. However, the main focus in this paper is on the interface treatment.

Assuming zero boundary data and forcing function F, the energy method leads to

$$\frac{\mathrm{d}}{\mathrm{d}t}\left(\|u_t\|^2 + \|u_x\|^2 + \beta u^2(1,t) - \alpha u^2(0,t)\right) = 0. \tag{7}$$

The problem have an energy estimate if

$$\alpha \leqslant 0, \quad \beta \geqslant 0. \tag{8}$$

The discrete boundary conditions corresponding to (6) can be written

$$L_l^{\mathrm{T}} v = (\alpha I l_N + I l_N S)v = g_l, \quad L_r^{\mathrm{T}} v = (\beta I r_N + I r_N S)v = g_r, \tag{9}$$

where v is the discrete solution vector, S is the boundary derivative operator in Definition 2.1, Il_N and Ir_N are defined in (1). The boundary conditions can be combined to $L^{\mathrm{T}} v = g(t)$, where $g(t) = [g_l(t) g_r(t)]^{\mathrm{T}}$ and $L = [L_l, L_r]$.

The projection method for the wave equation on second order form with the boundary conditions (6), can formally be written

$$\begin{aligned} &v_{tt} = PD_2 v + (I - P)\hat{g}_{tt}(t) + PF, \\ &v(0) = f_1, \quad v_t(0) = f_2, \end{aligned} \tag{10}$$

where $\hat{g}(t) = [g_l(t), 0, \ldots, 0, g_r(t)]^{\mathrm{T}}$, I the identity matrix and P the projection operator, given by

$$P = I - H^{-1}L(L^{\mathrm{T}}H^{-1}L)^{-1}L^{\mathrm{T}}. \tag{11}$$

In [24], it is proved that the following holds for the projection P,

$$\begin{aligned}
&\text{(i)} \quad (I-P)(v(t)-\hat{g}(t)) = (I-P)(f_1-\hat{g}(0)),\\
&\text{(ii)} \quad P^2 = P,\\
&\text{(iii)} \quad v = Pv + (I-P)\hat{g}(t) \Longleftrightarrow L^{\mathrm{T}}v = g(t),\\
&\text{(iv)} \quad HP = P^{\mathrm{T}}H.
\end{aligned} \tag{12}$$

The first property in (12) means that the solution to (10) will satisfy the BC only if the boundary data and the initial data are consistent.

When we solve (10) numerically we have to compute the second derivative of $\hat{g}(t)$, if we have time dependent boundary data. To avoid this we make the substitution $w = v - (I-P)\hat{g}(t)$ and get the following system of ordinary differential equations (ODE) for w

$$\begin{aligned}
&w_{tt} = PD_2w - PD_2(I-P)\hat{g}(t) + PF,\\
&w(0) = f_1 - (I-P)\hat{g}(0), \quad w_t(0) = f_2 - (I-P)\hat{g}_t(0).
\end{aligned} \tag{13}$$

Thus to solve for v numerically we solve (13) for w and then compute $v = w + (I-P)\hat{g}(t)$. In the numerical examples through out this paper we will consider homogeneous boundary data and forcing function. Strict stability for non-homogeneous boundary conditions are obtained in a straight forward manner, as shown in [24].

Lemma 3.1. *The problem (10) with $\hat{g} = 0$ and $F = 0$ have a non-growing solution if D_2 is an SBP operator with $A = A^{\mathrm{T}}$, and (8) holds.*

Proof. If F, $\hat{g} = 0$ and if D_2 is an SBP operator, the energy method applied to (10) leads to

$$\begin{aligned}
v_t^{\mathrm{T}}Hv_{tt} + v_{tt}^{\mathrm{T}}Hv_t &= -(Pv_t)^{\mathrm{T}}A(v) - (v)^{\mathrm{T}}A^{\mathrm{T}}(Pv_t) - 2(Pv_t)_0(Sv)_0 + 2(Pv_t)_N(Sv)_N\\
&= -(v_t)^{\mathrm{T}}A(v) - (v)^{\mathrm{T}}A^{\mathrm{T}}(v_t) + 2\alpha(v_t)_0v_0 - 2\beta(v_t)_Nv_N.
\end{aligned}$$

In the first step we use the fourth property in (12) together with the SBP property (see Definition 2.1) and in the last step we use (9) together with the third property. If A is symmetric, we obtain

$$\frac{\mathrm{d}}{\mathrm{d}t}(\|v_t\|_H^2 + v^{\mathrm{T}}Av + \beta v_N^2 - \alpha v_0^2) = 0.$$

This is completely analogous to (7). If (8) holds we have a non-growing energy. □

Due to Lemma 3.1 we introduce yet another definition (compare with Definition 2.1).

Definition 3.2. A difference operator $H^{-1}(-A+BS)$ approximating $\partial^2/\partial x^2$ is said to be a symmetric second derivative SBP operator if it is an SBP operator and if $A = A^{\mathrm{T}}$.

In [20] we constructed compact and symmetric second derivative SBP operators of order 4, 6 and 8. The second and sixth order accurate operators (presented in Appendix II) have been used for the computations in Section 6.

3.2. Media interface

We start by deriving the interface conditions for the continuous problem. Consider the wave equation

$$a^{-1}w_{tt} = (bw_x)_x, \qquad x \in [-1,1], \quad t \geqslant 0,$$

where $a, b > 0$ are discontinuous at $x = 0$ and $c = \sqrt{ab}$ is the wave propagation speed. Integration by parts leads to

$$\begin{aligned}
\int_{-1}^{1} a^{-1}w_{tt}w_t\,\mathrm{d}x &= \lim_{\epsilon\to 0}\left(\int_{-1}^{-\epsilon}(bw_x)_xw_t\,\mathrm{d}x - \int_{1}^{\epsilon}(bw_x)_xw_t\,\mathrm{d}x\right)\\
&= \lim_{\epsilon\to 0}\left(bw_xw_t|_{-1}^{1} - bw_xw_t|_{-\epsilon}^{\epsilon} - \int_{-1}^{-\epsilon}bw_xw_{xt}\,\mathrm{d}x + \int_{1}^{\epsilon}bw_xw_{xt}\,\mathrm{d}x\right).
\end{aligned}$$

To obtain an energy estimate require that w and b w_x are continuous across the interface, i.e., $\lim_{\epsilon\to 0}(bw_xw_t|_{-\epsilon}^{\epsilon}) = 0$, leading to $\frac{d}{dt}(\|w_t\|^2_{a^{-1}} + \|w_x\|^2_b) = bw_xw_t|_{-1}^{1}$. From now on we assume that a and b are piecewise constant, leading to the following system:

$$\begin{aligned} a_1^{-1}u_{tt} &= b_1u_{xx}, \quad -1 \leqslant x \leqslant 0, \\ a_2^{-1}v_{tt} &= b_2v_{xx}, \quad 0 \leqslant x \leqslant 1, \end{aligned} \tag{14}$$

where $a_1 \neq a_2$, $b_1 \neq b_2$. Continuity at the interface ($x = 0$) means that

$$u = v, \quad b_1u_x = b_2v_x. \tag{15}$$

If we use the interface conditions (15) and apply homogeneous Neumann conditions ($u_x = 0$) at the outer boundaries the energy method leads to

$$\frac{d}{dt}E = 0, \tag{16}$$

where the energy is defined as

$$E = a_1^{-1}\|u_t\|^2 + a_2^{-1}\|v_t\|^2 + b_1\|u_x\|^2 + b_2\|v_x\|^2. \tag{17}$$

We will treat the semi-discrete problem in such a way that we exactly mimic (16).

The projection method for the problem (14) and (15) can formally be written

$$PA^{-1}w_{tt} = PDw, \tag{18}$$

where $D = \mathrm{diag}(b_1D_2^{(l)}, b_2D_2^{(r)})$, $w = [u, v]^T$ and $A^{-1} = \mathrm{diag}(a_1^{-1}I_{N_l}, a_2^{-1}I_{N_r})$. Here u and v are the solution vectors corresponding to the left and right domain, respectively. The left and right domain is discretized using $(N_l + 1)$ and $(N_r + 1)$ grid points. The left and right boundary points of u and v will be denoted $w_{(\mathrm{LW,LI})}$ and $w_{(\mathrm{RI,RE})}$, respectively (see Fig. 2).

Remark. We can have different discretizations in the left and right domains. The only requirement for the stability analysis to hold is that we use symmetric SBP operators (see Definition 3.2) in each of the domains.

The projection operator is given by (11), where $H = \mathrm{diag}(H^{(l)}, H^{(r)})$ and the boundary operator have three parts

$$L = [L_{bl}L_{br}L_I], \tag{19}$$

where L_{bl}, L_{br} are the left and right boundary operators and L_I the interface operator approximating (15). To help define the total boundary operator (making use of (1)) we introduce

$$L_l^T = [Il_{N_l}S^{(l)}], \quad L_r^T = [Ir_{N_r}S^{(r)}], \tag{20}$$

corresponding to the left and right boundary and

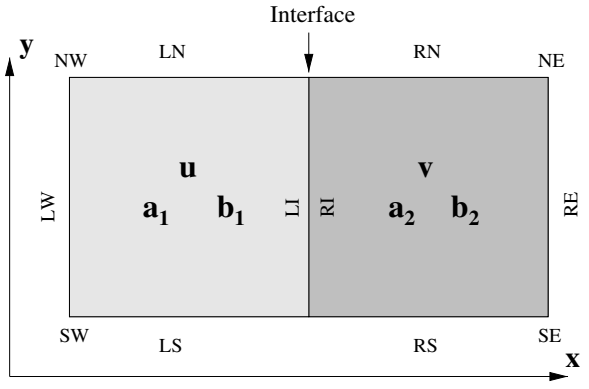

Fig. 2. Domain 2-D media discontinuity.

$$L_{Il}^{\mathrm{T}} = [b_1 Ir_{N_l} S^{(l)}; Ir_{N_l}], \quad L_{Ir}^{\mathrm{T}} = [b_2 Il_{N_r} S^{(r)}; Il_{N_r}], \tag{21}$$

corresponding to the left and right interface. Here the semicolon ; means row separation in a matrix (MATLAB notation, for those familiar with that). For example, $L_l^{\mathrm{T}} u = (S^{(l)} u)_0 \sim (u_x)_0$, i.e., a difference approximation of the left boundary derivative. The boundary and interface operators are given by

$$L_{bl}^{\mathrm{T}} = [L_l^{\mathrm{T}} L_0^{\mathrm{T}}], \quad L_{br}^{\mathrm{T}} = [L_0^{\mathrm{T}} L_r^{\mathrm{T}}], \quad L_I^{\mathrm{T}} = [L_{Il}^{\mathrm{T}} - L_{Ir}^{\mathrm{T}}], \tag{22}$$

where L_0^{T} is a zero vector of appropriate dimension.

If we multiply (18) by $w_t^{\mathrm{T}} H$ we obtain

$$w_t^{\mathrm{T}} HPA^{-1} w_{tt} - w_t^{\mathrm{T}} HPDw = w_t^{\mathrm{T}} HA^{-1} w_{tt} - w_t^{\mathrm{T}} HDw = 0$$

by using the third and fourth properties in (11). By adding the transpose we obtain an energy estimate (not shown here) completely analogous to (16), assuming that $D_2^{(lr)}$ are symmetric SBP operators (see Definition 3.2) based on diagonal norms (which is true for the operators used in this paper, see Appendix II). However, to obtain a well-defined left hand side for the ODE system (18) requires that $PA^{-1} w_{tt} = A^{-1} P w_{tt} (= A^{-1} w_{tt})$, since P is singular. Hence, in order to solve (18), it is necessary that the following condition holds:

$$PA^{-1} = A^{-1} P. \tag{23}$$

For a general P this expresses a compatibility condition between the analytic interface conditions (15) and the coefficient a^{-1}. For the problem (14) and (15), P is given by (11) and (19). Condition (23) certainly holds if a^{-1} is constant in a neighborhood of $x = 0$, such that $\mathrm{diag}(A^{-1})$ is constant at the $r + 1$ number of grid-points used by the boundary derivative operators $S^{(l,r)}$ (see Appendix II). In this paper (23) does not hold since a^{-1} is discontinuous at the interface.

Remark. A strictly stable overall discretization (considering both time and space discretization) requires (23) to hold. By computing the eigenvalues to the semi-discrete approximation (18) under the false assumption that (23) holds, we found that we do obtain strictly stable approximations for the 2nd and 6th order discretizations even with a variable a^{-1}, discontinuous at the interface. However, we also found examples where the corresponding 8th order approximation leads to an unstable approximation using (18) and a discontinuous a^{-1}.

To avoid the compatibility condition (23) we will transform the original continuous problem (14), (15) and derive an estimate for the transformed problem that will lead to a discrete energy estimate. We then transform back to the original problem. Consider the continuous problem:

$$\begin{aligned} \tilde{u}_{tt} &= c_1^2 \tilde{u}_{xx}, \quad -1 \leqslant x \leqslant 0, \\ \tilde{v}_{tt} &= c_2^2 \tilde{v}_{xx}, \quad 0 \leqslant x \leqslant 1, \end{aligned} \tag{24}$$

where we introduce the notation $c_k = a_k b_k$, $k = 1, 2$. We introduce a modified energy (compare with (17))

$$\widetilde{E} = \|\tilde{u}_t\|^2 + \|\tilde{v}_t\|^2 + c_1^2 \|\tilde{u}_x\|^2 + c_2^2 \|\tilde{v}_x\|^2. \tag{25}$$

The energy method on (24) leads to

$$\frac{\mathrm{d}}{\mathrm{d}t} \widetilde{E} = c_1^2 \tilde{u}_x \tilde{u}_t \big|_{-1}^{0} - c_2^2 \tilde{v}_x \tilde{v}_t \big|_{1}^{0}.$$

The following condition: $c_1^2 \tilde{u}_x \tilde{u}_t = c_2^2 \tilde{v}_x \tilde{v}_t$ at $x = 0$, is required to obtain an energy estimate. We consider (15), i.e., $\tilde{u} = \tilde{v}$ and $b_1 \tilde{u}_x = b_2 \tilde{v}_x$ to be the correct interface conditions (considering the physics). However, applying (15) for the energy (25) does not lead to a energy estimate (since the right hand side is indefinite).

By introducing the scaling (and assuming piecewise constant coefficients)

$$u = \sqrt{a_1}\tilde{u}, \quad v = \sqrt{a_2}\tilde{v} \tag{26}$$

into the original problem (14) and (15), we obtain (24) and the modified interface conditions

$$\sqrt{a_1}\tilde{u} = \sqrt{a_2}\tilde{v}, \quad b_1 \sqrt{a_1} \tilde{u}_x = b_2 \sqrt{a_2} \tilde{v}_x. \tag{27}$$

With homogeneous Neumann boundary conditions, the modified continuous problem (24) and (27) leads to the energy estimate

$$\frac{\mathrm{d}}{\mathrm{d}t}\widetilde{E} = 0. \tag{28}$$

The estimate (28) is completely analogous to (16), i.e., the modified energy (25) transforms to (17). This can be seen by using (26) to transform back to the original set of variables. The projection method applied to the modified problem (24) and (27) leads to

$$\tilde{w}_{tt} = \widetilde{P}\widetilde{D}\tilde{w}, \tag{29}$$

where $\widetilde{D} = \mathrm{diag}(c_1^2 D_2^{(l)}, c_2^2 D_2^{(r)})$ and $\tilde{w} = [\tilde{u}, \tilde{v}]^{\mathrm{T}}$. The modified projection operator $\widetilde{P}$ is given by (11) and (19) where now (instead of (21))

$$L_{Il}^{\mathrm{T}} = [b_1\sqrt{a_1} Ir_{N_l} S^{(l)}; \sqrt{a_1} IIr_{N_l}], \quad L_{Ir}^{\mathrm{T}} = [b_2\sqrt{a_2} IIl_{N_r} S^{(r)}; \sqrt{a_2} IIl_{N_r}]. \tag{30}$$

We introduce a discrete analog to (17), given by

$$E_H = a_1^{-1}\|u_t\|_{H^{(l)}} + a_2^{-1}\|v_t\|_{H^{(r)}} + b_1 u^{\mathrm{T}} A^{(l)} u + b_2 v^{\mathrm{T}} A^{(r)} v. \tag{31}$$

Lemma 3.3. *If $D_2^{(l,r)}$ are symmetric second derivative SBP operators, (29) is a strictly stable approximation to (14).*

Proof. The energy method on (29) leads to

$$\begin{aligned}
&\tilde{w}_t^{\mathrm{T}}\overline{H}\tilde{w}_{tt} + \tilde{w}_{tt}^{\mathrm{T}}\overline{H}\tilde{w}_t + (\widetilde{P}\tilde{w}_t)^{\mathrm{T}}\overline{A}(\tilde{w}) + (\tilde{w})\overline{A}^{\mathrm{T}}(\widetilde{P}\tilde{w}_t) \\
&\quad = 2(\widetilde{P}\tilde{w}_t)(\overline{BS}\tilde{w}) = -2c_1^2(\widetilde{P}\tilde{w}_t)_{(\mathrm{LW})}(S\tilde{w})_{(\mathrm{LW})} + 2c_1^2(\widetilde{P}\tilde{w}_t)_{(\mathrm{LI})}(S\tilde{w})_{(\mathrm{LI})} \\
&\qquad\qquad - 2c_2^2(\widetilde{P}\tilde{w}_t)_{(\mathrm{RI})}(S\tilde{w})_{(\mathrm{RI})} + 2c_2^2(\widetilde{P}\tilde{w}_t)_{(\mathrm{RE})}(S\tilde{w})_{(\mathrm{RE})} = 0,
\end{aligned}$$

where $\overline{H} = \mathrm{diag}(H^{(l)}, H^{(r)})$, $\overline{A} = \mathrm{diag}(c_1^2 A^{(l)}, c_2^2 A^{(r)})$, $\overline{B} = \mathrm{diag}(B^{(l)}, B^{(r)})$ and $\overline{S} = \mathrm{diag}(c_1^2 S^{(l)}, c_2^2 S^{(r)})$. The left and right boundary points of $\tilde{u}$ and $\tilde{v}$ are denoted by $\tilde{w}_{(\mathrm{LW,LI})}$ and $\tilde{w}_{(\mathrm{RI,RE})}$, respectively (see Fig. 2). In the first step we use the fourth property in (12) and in the second step we use the SBP property (see Definition 2.1). In the last step we utilize the fact that we apply (through the projection) homogenous Neumann BC and the interface conditions (27) via the third property in (12), i.e., $c_1^2(\widetilde{P}\tilde{w}_t)_{(\mathrm{LI})}(S\tilde{w})_{(\mathrm{LI})} = c_2^2(\widetilde{P}\tilde{w}_t)_{(\mathrm{RI})}(S\tilde{w})_{(\mathrm{RI})}$, $(\widetilde{P}\tilde{w}_t)_{(\mathrm{RE})}(S\tilde{w})_{(\mathrm{RE})} = 0$ and $(\widetilde{P}\tilde{w}_t)_{(\mathrm{LW})}(S\tilde{w})_{(\mathrm{LW})} = 0$.

If $A^{(l,r)}$ are symmetric we obtain the following energy estimate:

$$\frac{\mathrm{d}}{\mathrm{d}t}E_H = 0,$$

by utilizing (26) to go back to the original set of variables. The energy is defined in (31). This estimate is completely analogous to (16), which means that (29) is a strictly stable approximation. □

Remark. We have not found a way around the compatibility condition (23), except for the case of piecewise constant coefficients. One way around the restriction to piecewise constant coefficients, i.e., condition (23), is to utilize the SAT method at the interface. This will be pursued in a coming paper.

4. The projection method in 2-D

We extend the analysis to two-dimensional, rectangular domains and show that the projection method requires special treatment at corners.

4.1. Single domain

Consider the two-dimensional wave equation

$$\begin{aligned} &a^{-1}u_{tt} = b\left(u_{xx} + u_{yy}\right), \qquad -1 \leqslant x \leqslant 1, \quad 0 \leqslant y \leqslant 1,\\ &u_x = 0, \qquad x = -1, 1, \quad 0 \leqslant y \leqslant 1,\\ &u_y = 0, \qquad -1 \leqslant x \leqslant 1, \quad y = 0, 1. \end{aligned} \tag{32}$$

To simplify notation in this section we set $a = b = 1$. The energy method leads to

$$\frac{\mathrm{d}}{\mathrm{d}t}(\|u_t\|^2 + \|u_x\|^2 + \|u_y\|^2) = 0. \tag{33}$$

A semi-discrete approximation to (32) using the Projection method can formally be written

$$v_{tt} = P((D_2)_x \otimes I_M + I_N \otimes (D_2)_y)v, \tag{34}$$

where we have simplified the notation by using the Kronecker product introduced in Section 2. The projection operator is given by (11) where the norm is defined as $H = (H_x \otimes I_M)(I_N \otimes H_y)$ and $I = I_N \otimes I_M$. The presence of corners introduce a complication, when Neumann boundary conditions are used. Consider the boundary operator

$$\widetilde{L} = [\, L_{\mathrm{W}} \quad L_{\mathrm{N}} \quad L_{\mathrm{E}} \quad L_{\mathrm{S}} \,] \in \mathbf{R}^{(N+1)\times(M+1)\times 2(N+M+2)} \tag{35}$$

with contributions from the four sides (west, north, east and south), where $L_{\mathrm{W}}^{\mathrm{T}} = L_l^{\mathrm{T}} \otimes I_M$, $L_{\mathrm{N}}^{\mathrm{T}} = I_N \otimes L_r^{\mathrm{T}}$, $L_{\mathrm{E}}^{\mathrm{T}} = L_r^{\mathrm{T}} \otimes I_M$, $L_{\mathrm{S}}^{\mathrm{T}} = I_N \otimes L_l^{\mathrm{T}}$, and $L_{l,r}^{\mathrm{T}}$ are defined in (20). By using the notation from Section 2 (see also Fig. 1) the boundary operators at the four sides are defined through

$$\begin{aligned} &L_{\mathrm{S}}^{\mathrm{T}} v = (Sv)_{\mathrm{S}} = (Sv)_{i,0} = 0, \quad i = 0, \ldots, N,\\ &L_{\mathrm{W}}^{\mathrm{T}} v = (Sv)_{\mathrm{W}} = (Sv)_{0,j} = 0, \quad j = 0, \ldots, M,\\ &L_{\mathrm{N}}^{\mathrm{T}} v = (Sv)_{\mathrm{N}} = (Sv)_{i,M} = 0, \quad i = 0, \ldots, N,\\ &L_{\mathrm{E}}^{\mathrm{T}} v = (Sv)_{\mathrm{E}} = (Sv)_{N,j} = 0, \quad j = 0, \ldots, M. \end{aligned}$$

The boundary condition $\widetilde{L}^{\mathrm{T}} v = 0$ (including all boundary points) imply that two boundary conditions are prescribed at each of the four corners, see Fig. 1.

Remark. A well-defined projection operator P requires a boundary operator L that (i) covers all boundary points, and (ii) have full rank, i.e., no linear dependence.

The total number of prescribed boundary conditions in (35) are $2(N+1) + 2(M+1)$. Thus, the projection operator is well defined iff $\mathrm{rank}(\widetilde{L}) = 2(N+M+2)$. However, in [24] it is shown that L constructed in this way is linearly dependent, and that the corner points requires special treatment.

In the following lemma we make use of the point-wise boundary operators ($(L_{\mathrm{S}})_i$, $(L_{\mathrm{W}})_j$, $(L_{\mathrm{N}})_i$ and $(L_{\mathrm{E}})_j$) defined through

$$(L_{\mathrm{S}}^{\mathrm{T}} v)_i = (Sv)_{i,0}, \quad (L_{\mathrm{W}}^{\mathrm{T}} v)_i = (Sv)_{0,j}, \quad (L_{\mathrm{N}}^{\mathrm{T}} v)_i = (Sv)_{i,M}, \quad (L_{\mathrm{E}}^{\mathrm{T}} v)_j = (Sv)_{N,j}$$

for $i = 0, \ldots, N$, $j = 0, \ldots, M$, where

$$\begin{aligned} (L_{\mathrm{S}}^{\mathrm{T}})_i &= \frac{1}{h_y}\left[0 \ldots 0 \sum_{k=0}^{M} s_k e_k^{\mathrm{T}} 0 \ldots 0\right],\\ (L_{\mathrm{W}}^{\mathrm{T}})_j &= \frac{1}{h_x}[s_0 e_j^{\mathrm{T}} \ldots, s_N e_j^{\mathrm{T}} 0 \ldots 0],\\ (L_{\mathrm{N}}^{\mathrm{T}})_i &= \frac{1}{h_y}\left[0 \ldots 0 - \frac{1}{h_y}\sum_{k=0}^{M} s_{M-k} e_k^{\mathrm{T}} 0 \ldots 0\right], \end{aligned}$$

$$(L_{\mathrm{E}}^{\mathrm{T}})_j = \frac{1}{h_x}[0\ldots 0 s_N e_j^{\mathrm{T}} \ldots, s_0 e_j^{\mathrm{T}}] \tag{36}$$

and $\{e_j\}$ is a canonical basis in R^{N+1}. For example,

$$(L_{\mathrm{S}}^{\mathrm{T}})_0 = \frac{1}{h_y}[s_0 s_1 \ldots s_M 0 \ldots 0] \in \mathbf{R}^{1\times(M+1)(N+1)},$$

$$(L_{\mathrm{W}}^{\mathrm{T}})_0 = \frac{1}{h_x}[s_0 0 \ldots 0 s_1 0 \ldots 0 \ldots s_N 0 \ldots 0] \in \mathbf{R}^{1\times(M+1)(N+1)}$$

are the boundary operators in the y- and x-direction, respectively, at grid-point $(0,0)$, i.e., at SW in Fig. 1.

Remark. Note that $s_k = 0$, for $k > r+1$, where $r+1$ is the number of grid points defining the boundary derivative S. For the sixth order approximation $r = 4$, see Appendix II.

To have a well-defined projection (11), it is necessary to reduce the number of boundary conditions to one at each corner. We follow the procedure in [24] and construct a new boundary operator by forming linear combinations (see Fig. 1)

$$L_{\mathrm{SW}}^{\mathrm{T}} = (1-\eta_{\mathrm{SW}})(L_{\mathrm{S}}^{\mathrm{T}})_0 + \eta_{\mathrm{SW}}(L_{\mathrm{W}}^{\mathrm{T}})_0, \quad L_{\mathrm{NW}}^{\mathrm{T}} = (1-\eta_{\mathrm{NW}})(L_{\mathrm{N}}^{\mathrm{T}})_0 + \eta_{\mathrm{NW}}(L_{\mathrm{W}}^{\mathrm{T}})_N,$$
$$L_{\mathrm{NE}}^{\mathrm{T}} = (1-\eta_{\mathrm{NE}})(L_{\mathrm{N}}^{\mathrm{T}})_N + \eta_{\mathrm{NE}}(L_{\mathrm{E}}^{\mathrm{T}})_N, \quad L_{\mathrm{SE}}^{\mathrm{T}} = (1-\eta_{\mathrm{SE}})(L_{\mathrm{S}}^{\mathrm{T}})_N + \eta_{\mathrm{SE}}(L_{\mathrm{E}}^{\mathrm{T}})_0,$$

where $0 \leqslant \eta_{\mathrm{SW}}, \eta_{\mathrm{NW}}, \eta_{\mathrm{NE}}, \eta_{\mathrm{SE}} \leqslant 1$. The final boundary operator is given by

$$L = [\,L_{\mathrm{S}} \quad L_{\mathrm{W}} \quad L_{\mathrm{N}} \quad L_{\mathrm{E}} \quad L_{\mathrm{SW}} \quad L_{\mathrm{NW}} \quad L_{\mathrm{NE}} \quad L_{\mathrm{SE}}\,] \in R^{(N+1)\times(M+1)\times 2(N+M)}. \tag{37}$$

The modified side operators are given by

$$L_{\mathrm{S}}^{\mathrm{T}} = I\!I_M \otimes L_l^{\mathrm{T}}, \quad L_{\mathrm{W}}^{\mathrm{T}} = L_l^{\mathrm{T}} \otimes I\!I_N, \quad L_{\mathrm{N}}^{\mathrm{T}} = I\!I_M \otimes L_r^{\mathrm{T}}, \quad L_{\mathrm{E}}^{\mathrm{T}} = L_r^{\mathrm{T}} \otimes I\!I_N,$$

thus excluding the corner points, see (1). The total number of boundary conditions are now reduced to $2(N+M)$, and equals the total number of boundary points. The following lemma shows how to obtain a well-defined boundary operator for a two-dimensional problem with Neumann boundary conditions.

Lemma 4.1. *The columns of L in (37) are linearly independent and* $\mathrm{Rank}(L) = 2(N+M)$, *leading to a well-defined projection, iff* $\eta_{\mathrm{NW}}, \eta_{\mathrm{SE}} \neq \frac{h_x}{h_x+h_y}$.

The proof is given in Appendix I.

We are now ready to tie everything together in the following proposition.

Proposition 4.2. *The semi-discrete approximation (34) is strictly stable if D_2 is a symmetric SBP operator (see Definition 3.2), the boundary operator is given by (37) and* $\eta_{\mathrm{NW}}, \eta_{\mathrm{SE}} \neq \frac{h_x}{h_x+h_y}$.

Proof. The energy method applied to (34) yields

$$\frac{\mathrm{d}}{\mathrm{d}t}(\|v_t\|_H^2 + v^{\mathrm{T}}(H^{(x)} \otimes A^{(y)})v + v^{\mathrm{T}}(A^{(x)} \otimes H^{(y)})v) = (Pv_t)_{(N)}^{\mathrm{T}} H^{(x)}(Sv)_{(N)} - (Pv_t)_{(S)}^{\mathrm{T}} H^{(x)}(Sv)_{(S)}$$
$$+ (Pv_t)_{(E)}^{\mathrm{T}} H^{(y)}(Sv)_{(E)} - (Pv_t)_{(W)}^{\mathrm{T}} H^{(y)}(Sv)_{(W)} = 0,$$

where $v_{(\mathrm{N,S,E,W})}$ symbolizes the boundary vectors at the north, south, east and west boundaries, respectively, see Fig. 1. In the first step we use the fourth property in (12) and the symmetric SBP property (see Definition 3.2). In the last step we utilize the fact that we apply (through the projection) homogenous Neumann BC, together with the third property in (12), i.e., $(Pv_t)_{(\mathrm{N,S})}^{\mathrm{T}} H^{(x)}(Sv)_{(\mathrm{N,S})} = 0$ and $(Pv_t)_{(\mathrm{W,E})}^{\mathrm{T}} H^{(y)}(Sv)_{(\mathrm{W,E})} = 0$.

Hence, if D_2 is a symmetric SBP operator and if the boundary operator (37) is well defined, i.e., if $\eta_{\mathrm{NW}}, \eta_{\mathrm{SE}} \neq \frac{h_x}{h_x+h_y}$ as shown in Lemma 4.1, we obtain an energy estimate completely analogous to (33). This means that (34) is a strictly stable approximation to (32). □

4.2. Media interface

Consider the wave equation

$$\begin{aligned} a_1^{-1}u_{tt} &= b_1(u_{xx}+u_{yy}), \quad x\in[-1,0], y\in[0,1],\\ a_2^{-1}v_{tt} &= b_2(v_{xx}+v_{yy}), \quad x\in[0,+1], y\in[0,1] \end{aligned} \tag{38}$$

on two different media $b_1 \neq b_2$ and $a_1 \neq a_2$ (see Fig. 2) with the interface conditions given by (15) and Neumann boundary conditions. The energy method leads to

$$\frac{\mathrm{d}}{\mathrm{d}t}(a_1^{-1}\|u_t\|^2 + a_2^{-1}\|v_t\|^2 + b_1(\|u_x\|^2+\|u_y\|^2) + b_2(\|v_x\|^2+\|v_y\|^2)) = 0. \tag{39}$$

The semi-discrete approximation (again utilizing the transformation (26)) using the projection method, can formally be written

$$w_{tt} = P(D_x + D_y)w, \tag{40}$$

where $w=[\tilde{u},\tilde{v}]^{\mathrm{T}}$, $D_x = \mathrm{diag}(c_1^2 D_2^{(l)}\otimes I_M, c_2^2 D_2^{(r)}\otimes I_M)$ and $D_y = \mathrm{diag}(I_{N_l}\otimes c_1^2 D_2^{(l)}, I_{N_r}\otimes c_2^2 D_2^{(r)})$. To simplify notation in this section we skip the tilde signs over w and P.

The projection operator is given by (11), where $H = \mathrm{diag}(H_x^{(l)}\otimes I_M, H_x^{(r)}\otimes I_M)\times \mathrm{diag}(I_{N_l}\otimes H_y^{(l)}, I_{N_r}\otimes H_y^{(r)})$ and the boundary operator

$$L = [\,L_{\mathrm{LS}} \quad L_{\mathrm{SW}} \quad L_{\mathrm{LW}} \quad L_{\mathrm{NW}} \quad L_{\mathrm{LN}} \quad L_{\mathrm{RN}} \quad L_{\mathrm{NE}} \quad L_{\mathrm{RE}} \quad L_{\mathrm{SE}} \quad L_{\mathrm{RS}} \quad L_I\,].$$

The side operators are defined as:

$$\begin{aligned} L_{\mathrm{LS}}^{\mathrm{T}} &= [IL_{N_l}\otimes L_l^{\mathrm{T}}L_0^{\mathrm{T}}], \quad L_{\mathrm{LW}}^{\mathrm{T}} = [L_l^{\mathrm{T}}\otimes IH_M L_0^{\mathrm{T}}], \quad L_{\mathrm{LN}}^{\mathrm{T}} = [IL_{N_l}\otimes L_r^{\mathrm{T}}L_0^{\mathrm{T}}],\\ L_{\mathrm{RN}}^{\mathrm{T}} &= [L_0^{\mathrm{T}}IR_{N_r}\otimes L_r^{\mathrm{T}}], \quad L_{\mathrm{RE}}^{\mathrm{T}} = [L_0^{\mathrm{T}}L_r^{\mathrm{T}}\otimes IH_M], \quad L_{\mathrm{RS}}^{\mathrm{T}} = [L_0^{\mathrm{T}}IR_{N_r}\otimes L_l^{\mathrm{T}}] \end{aligned}$$

complemented with the corner treatment (see Lemma 4.1):

$$\begin{aligned} L_{\mathrm{SW}}^{\mathrm{T}} &= (1-\eta_{\mathrm{SW}})[Il_{N_l}\otimes L_l^{\mathrm{T}}L_0^{\mathrm{T}}] + \eta_{\mathrm{SW}}[L_l^{\mathrm{T}}\otimes Il_M L_0^{\mathrm{T}}],\\ L_{\mathrm{NW}}^{\mathrm{T}} &= (1-\eta_{\mathrm{NW}})[Il_{N_l}\otimes L_r^{\mathrm{T}}L_0^{\mathrm{T}}] + \eta_{\mathrm{NW}}[L_l^{\mathrm{T}}\otimes Ir_M L_0^{\mathrm{T}}],\\ L_{\mathrm{SE}}^{\mathrm{T}} &= (1-\eta_{\mathrm{SE}})[L_0^{\mathrm{T}}Ir_{N_r}\otimes L_l^{\mathrm{T}}] + \eta_{\mathrm{SE}}[L_0^{\mathrm{T}}L_r^{\mathrm{T}}\otimes Il_M],\\ L_{\mathrm{NE}}^{\mathrm{T}} &= (1-\eta_{\mathrm{NE}})[L_0^{\mathrm{T}}Ir_{N_r}\otimes L_r^{\mathrm{T}}] + \eta_{\mathrm{NE}}[L_0^{\mathrm{T}}L_r^{\mathrm{T}}\otimes Ir_M]. \end{aligned}$$

Here we have utilized the Kronecker product and the one-dimensional boundary operators (20). L_0^{T} is a zero vector of appropriate dimension and the interface operator is given by

$$L_I^{\mathrm{T}} = [L_{Il}^{\mathrm{T}} - L_{Ir}^{\mathrm{T}}]\otimes IH_M, \tag{41}$$

where L_{Il}^{T} and L_{Ir}^{T} are given by (30).

Remark. To obtain a well-defined boundary operator L we must not specify to many boundary conditions at the four corners, as described in the previous section. We must also avoid to over specify at the locations (here two) where the interface meets the outer boundaries. There are several ways to accomplish this. Here we simply specify the outer boundary conditions at the two locations. Another well defined choice is to specify a linear combination between the interface and the boundary conditions.

The energy method applied to (40) leads to

$$\frac{\mathrm{d}}{\mathrm{d}t}(\|\tilde{u}_t\|_{H^{(l)}} + \|\tilde{v}_t\|_{H^{(r)}} + c_1^2(\tilde{u}^{\mathrm{T}}(H_x^{(l)}\otimes A_y^{(l)})\tilde{u} + \tilde{u}^{\mathrm{T}}(A_x^{(l)}\otimes H_y^{(l)})\tilde{u}) + c_2^2(\tilde{v}^{\mathrm{T}}(H_x^{(r)}\otimes A_y^{(r)})\tilde{v} + \tilde{v}^{\mathrm{T}}(A_x^{(r)}\otimes H_y^{(r)})\tilde{v})) = 0,$$

where we make use of the fourth property in (12) and the symmetric SBP property (see Definition 3.2). We also utilize the fact that we apply (through the projection) homogenous Neumann BC and the interface conditions (27), together with the third property in (12), i.e., that the boundary and interface terms cancel or become zero. By utilizing (26) to go back to the original set of variables, we obtain

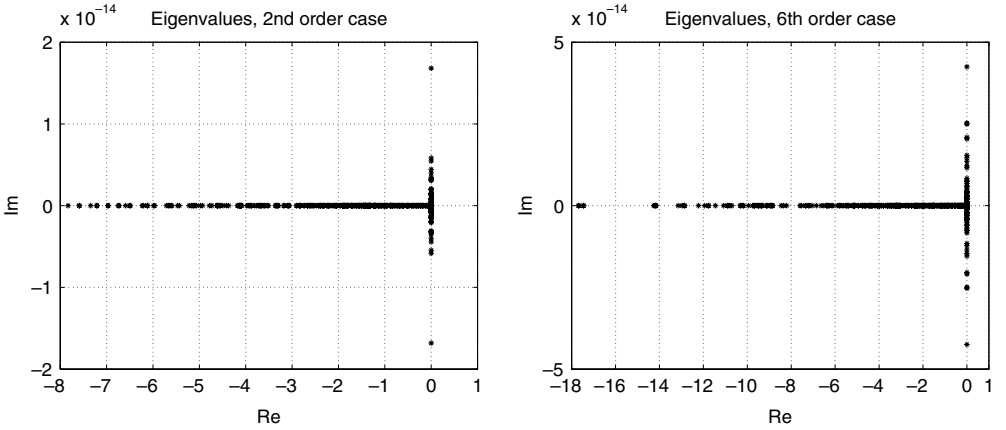

Fig. 3. The eigenvalues to $\widetilde{M}_{2,6}$ for the 2nd and 6th order discretizations (40), respectively, with $a_1 = b_1 = 1$, $a_2 = b_2 = 0.6$. $N = 2 \times 14^2$.

$$\frac{\mathrm{d}}{\mathrm{d}t}\left(a_1^{-1}\|u_l\|_{H_l} + a_2^{-1}\|v_l\|_{H_r} + b_1(u^{\mathrm{T}}(H_l^{(x)} \otimes A_l^{(y)})u + u^{\mathrm{T}}(A_l^{(x)} \otimes H_l^{(y)})u) + b_2(v^{\mathrm{T}}(H_r^{(x)} \otimes A_r^{(y)})v + v^{\mathrm{T}}(A_r^{(x)} \otimes H_r^{(y)})v)\right) = 0, \tag{42}$$

which is completely analogous to (39). This means that (40) is a strictly stable approximation.

Consider the ODE system $w_{tt} = Mw$, with the general solution

$$w = \sum_{k=0}^{N} \alpha_j \exp \sqrt{\beta_j} t,$$

where β_j are the eigenvalues to the matrix M and α_j the corresponding eigenvectors. If any of the eigenvalues have an imaginary and/or a positive real part we obtain exponential time-growth. The energy estimate (42) shows that the energy (and thus the solution) is bounded and that the eigenvalues to the operator $P(D_x + D_y)$ in (40) must be non-positive and real. This can be verified numerically by computing the eigenvalues to $h^2 P(D_x + D_y) = \widetilde{M}$. The result for the 2nd and 6th order discretizations of (40) with $a_1 = b_1 = 1$ and $a_2 = b_2 = 0.6$ are shown in Fig. 3.

5. Time integration

By combining symmetric second derivative SBP operators and the projection method, to implement the boundary and interface conditions (see for example (13), (29), (34) and (40)) we obtain an ODE system (with N unknowns):

$$\begin{aligned} &w_{tt} = Mw + G(t), \\ &w(0) = f_1, \quad w_t(0) = f_2 \end{aligned} \tag{43}$$

for the discrete solution vector w. Note that this form cannot be obtained by using the original formulation (18), since that requires (23) to hold. In Sections 3 and 4 we have shown that the matrix M have non-positive and real eigenvalues (a necessary stability condition) by utilizing the energy method.

To construct a compact and explicit high order accurate time marching method we start by introducing

$$w_{tt}^{(n)} = (D_+ D_-)^t w^{(n)} - \frac{k^2}{12} w_{tttt}^{(n)} - \frac{k^4}{360} w_{tttttt}^{(n)} + \mathcal{O}(k^6),$$

where $(D_+ D_-)^t$ is the central second order scheme in time, k the time step, and $t_n = nk$, $n = 0,1,\ldots$ By using (43) and Taylor expansions we can obtain a second order explicit time discretization:

$$\begin{aligned} &w^{(0)} = f_1, \quad w^{(1)} = f_1 + k f_2 + \tilde{f}_2, \\ &w^{(n+1)} - 2w^{(n)} + w^{(n-1)} = k^2 M w^{(n)} + \widetilde{G}_2^{(n)}, \quad n = 1, \ldots \end{aligned}$$

where $\tilde{f}_2 = (k^2/2)G$, at $t = 0$, and $\widetilde{G}_2^{(n)} = k^2 G$, at $t = t_n$.

A 6th order explicit time discretization is given by:

$$w^{(0)} = f_1, \quad w^{(1)} = \left(I_N + \frac{k^2}{2}M + \frac{k^4}{24}M^2\right)f_1 + k\left(I_N + \frac{k^2}{6}M + \frac{k^4}{120}M^2\right)f_2 + \tilde{f}_6,$$

$$w^{(n+1)} - 2w^{(n)} + w^{(n-1)} = k^2 M\left(I_N + \frac{k^2}{12}M + \frac{k^4}{360}M^2\right)w^{(n)} + \widetilde{G}_6^{(n)}, \quad n = 1, \ldots$$

where

$$\tilde{f}_6 = \frac{k^2}{2}G + \frac{k^3}{6}G_t + \frac{k^4}{24}(MG + G_{tt}) + \frac{k^5}{120}(MG_t + G_{ttt}) + \frac{k^6}{720}(M^2G + MG_{tt} + G_{tttt}), \quad t = 0$$

and

$$\widetilde{G}_6^{(n)} = k^2 G + \frac{k^4}{12}(MG + G_{tt}) + \frac{k^6}{360}(M^2G + MG_{tt} + G_{tttt}), \quad t = t_n.$$

The time marching method can formally be written

$$\begin{bmatrix} w^{(n+1)} \\ w^{(n)} \end{bmatrix} = \begin{bmatrix} C_p & -I_N \\ I_N & 0_N \end{bmatrix}\begin{bmatrix} w^{(n)} \\ w^{(n-1)} \end{bmatrix} + \begin{bmatrix} \widetilde{G}_p^{(n)} \\ 0_N \end{bmatrix}, \quad n = 1, \ldots$$

where 0_N is a zero $N \times N$-matrix and

$$C_2 = \alpha^2\widetilde{M} + 2I_N, \quad C_6 = \alpha^2\widetilde{M}\left(I_N + \frac{\alpha^2}{12}\widetilde{M} + \frac{\alpha^4}{360}\widetilde{M}^2\right) + 2I_N \tag{44}$$

for the 2nd and 6th order time discretizations, respectively. The CFL number is defined as

$$\alpha = \frac{k}{h_d}, \quad h_d = \sqrt{(h_x^2 + h_y^2)/2}$$

and $\widetilde{M} = h_d^2 M$ is the undivided operator. The stability requirement for the overall discretization is given by $\rho(C_{2,6}) \leqslant 2$, where the symbol ρ denotes the spectral radius. By utilizing (44) we obtain the following CFL conditions

$$\alpha \leqslant \frac{2}{\sqrt{\rho(\widetilde{M})}}, \quad \alpha \leqslant \frac{1.76}{\sqrt{\rho(\widetilde{M})}},$$

for the 2nd and 6th order time discretizations, respectively. By performing numerical simulations we found that the above estimates are sharp. Note that $\rho(\widetilde{M})$ is independent of N, but problem dependent.

For the one-dimensional problem (29) (with $a_1 = b_1 = 1$ and $a_2 = b_2 = 0.6$) we obtain $\rho(\widetilde{M}_2) = 4.00$ and $\rho(\widetilde{M}_6) = 10.76$ for the 2nd and 6th order spatial operators, respectively. For the two-dimensional problem (40) we obtain $\rho(\widetilde{M}_2) = 7.83$ and $\rho(\widetilde{M}_6) = 17.69$, see Fig. 3.

6. Computations

6.1. Efficiency

To test the convergence rate for the discretizations of (14), (38), and Neumann boundary conditions, we choose an analytic solution

$$u = \cos(w_1 c_1 t)\cos(w_1 x), \quad x \in [-1, 0], \ t \geqslant 0, \qquad w_1 = (2n+1)\pi, \quad m, n \in \mathbf{Z},$$

$$v = \cos(w_2 c_2 t)\cos(w_2 x), \quad x \in [0, 1], \ t \geqslant 0, \qquad w_2 = (2m+1)\pi, \quad c_2 = c_1\frac{w_1}{w_2}.$$

The convergence rate is calculated as

$$q = \log_{10}\left(\frac{\|w - w^{(h_1)}\|_h}{\|w - w^{(h_2)}\|_h}\right) \Big/ \log_{10}\left(\frac{h_1}{h_2}\right),$$

where w is the analytic solution and $w^{(h_1)}$ the corresponding numerical solution with grid size h_1. $\|w - w^{(h_1)}\|_h$ is the l_2-error. A convergence study is shown in Table 1, comparing the 2nd and the 6th order discretizations (both time and space) with $a_1 = b_1 = 1$, $a_2 = b_2 = 0.6$, $n = 1$ and $m = 2$. The 6th order discretization have a 3rd order accurate boundary closure. This leads to 5th order global accuracy, since we gain two orders of accuracy (see [28,20]) for second derivatives. The CFL conditions for the 2nd and 6th order discretizations are given by 0.71 and 0.47, respectively. By analyzing the discretization error we found that the spatial discretization error dominate for moderate grid resolutions ($N \leqslant 2 \times 200^2$) and time integrations ($t < 1000$). The conclusion is that the second order time discretization is sufficient for the applications considered in this paper.

To evaluate the efficiency of the higher order discretization we compared the number of unknowns $N_{2,6}$ for the 2nd and 6th order case, respectively, to obtain a solution with an l_2-error less than 0.001 after $t = 1$, $t = 10$ and $t = 30$. The efficiency for a d-dimensional problem is defined as the fraction between the total number of operations for the second as compared to the 6th order discretization, i.e., $E_d = \frac{3N_2^d\alpha_6}{7N_6^d\alpha_2}$. Here we take into account the slightly different CFL conditions for the 2nd and 6th order spatial discretizations, denoted by α_2 and α_6, respectively. Hence, a value E_d over one is in favor of the higher order discretization. The results are shown in Table 2. We clearly see an increase in E_d for high dimensions and long time integrations. For even lower values of the error tolerance, the gain would be even higher.

6.2. Application

As an illustration we consider the two-dimensional wave equation (with $c_1 = 1$, $c_2 = 0.5$ and Neumann boundary conditions) on the 9-block domain shown in Fig. 4. To test the accuracy of the interface treatment we performed a convergence study, shown in Table 3, comparing the 2nd and the 6th order discretizations. The solutions on the two coarsest grids are poorly resolved for both discretizations, which explains the low convergence rate for the sixth order case in the second row. According to theory we should obtain 5th order convergence for the 6th order case (as mentioned above). To obtain a confident measure on the rate of convergence requires (i) a fairly grid-converged reference solution, and (ii) solutions far from grid-convergence. The solution using the 6th order discretization on the $(3 \times 97)^2$ grid (used in Table 3) does not meet the second requirement, which could explain the slightly lower (than five) rate of convergence. As initial data we specify a Gaussian pulse, centered at $(x, y) = (-1.5, -1.5)$ (see Fig. 4), away from any boundaries or interfaces. The solution is then advanced and recorded at $t = 1$ (see Fig. 5), when the pulse have

Table 1
log(l_2-error) and convergence, comparing the 6th to the 2nd order discretization, with $a_1 = b_1 = 1$, $a_2 = b_2 = 0.6$

N	$l_2^{(6th)}$	$q^{(6th)}$	$l_2^{(2nd)}$	$q^{(2nd)}$
2×26^2	−0.72		−0.33	
2×51^2	−2.15	4.89	−1.21	3.01
2×101^2	−3.64	5.02	−2.09	2.96
2×201^2	−5.14	5.03	−2.94	2.84

Table 2
Efficiency measurement, comparing the 6th to the 2nd order discretization

Time	$N_1^{(6th)}$	$N_1^{(2nd)}$	E_1	E_2	E_3
$t = 1$	43	111	0.66	1.71	4.42
$t = 10$	64	290	1.17	5.28	23.9
$t = 30$	95	570	1.54	9.26	55.5

N_1 in each dimension. $a_1 = b_1 = 1$, $a_2 = b_2 = 0.6$.

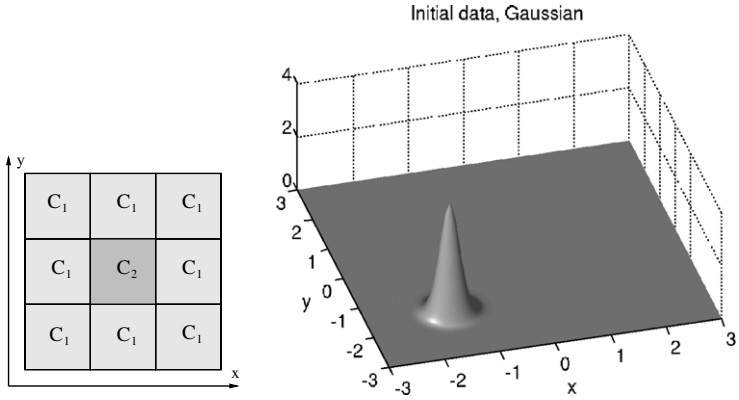

Fig. 4. Computational domain and initial solution, a Gaussian pulse.

Table 3
$\log(l_2$-error) and convergence, comparing the 6th to the 2nd order discretization, with $b_1 = c_1 = 1$, $b_2 = c_2 = 0.5$

N	$l_2^{(6th)}$	$q^{(6th)}$	$l_2^{(2nd)}$	$q^{(2nd)}$
$(3\times 13)^2$	−1.69	–	−1.80	–
$(3\times 25)^2$	−3.09	2.85	−2.52	1.51
$(3\times 49)^2$	−4.46	4.71	−3.20	2.40
$(3\times 97)^2$	−5.17	4.56	−3.83	2.25

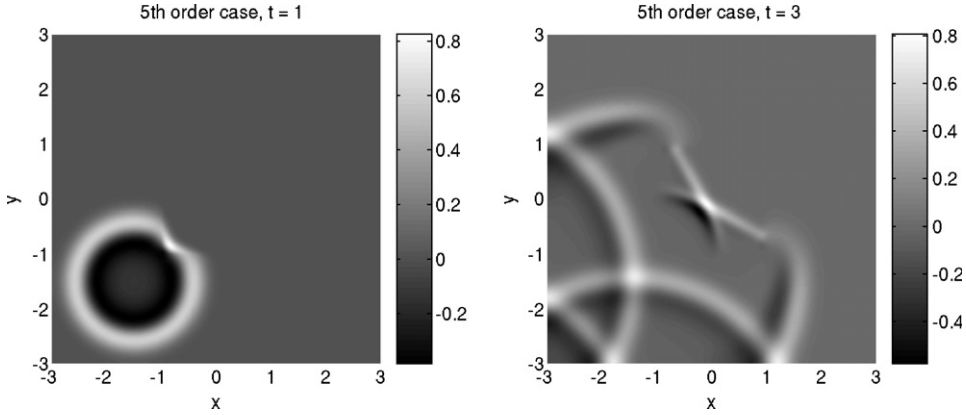

Fig. 5. Solution at $t = 1$ and $t = 3$. 6th order discretization and $N = (3\times 97)^2$ unknowns.

reached the lower left corner of the interface. At $t = 1$ the pulse have not yet influenced the outer boundaries. As a reference solution we use the 6th order accurate solution computed on a grid with $(3\times 385)^2$ unknowns.

The solutions at $t = 1$ and $t = 3$ using $N = (3\times 97)^2$ unknowns and the 6th order discretization are shown in Fig. 5. In Fig. 6 the solution at $t = 10$ is shown from two different perspectives. In Fig. 7 the errors at $t = 10$ are plotted, comparing the 2nd and 6th order discretizations. We use the 6th order solution on the $(3\times 385)^2$ grid as a reference solution. The discrete l_2 error for the 2nd and 6th order discretizations are 0.0123 and 0.00138, respectively.

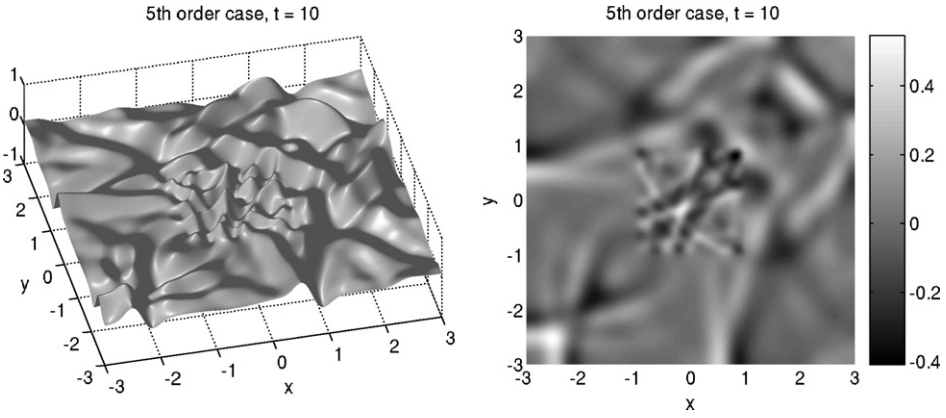

Fig. 6. Solution at $t = 10$. 6th order discretization. Two different views.

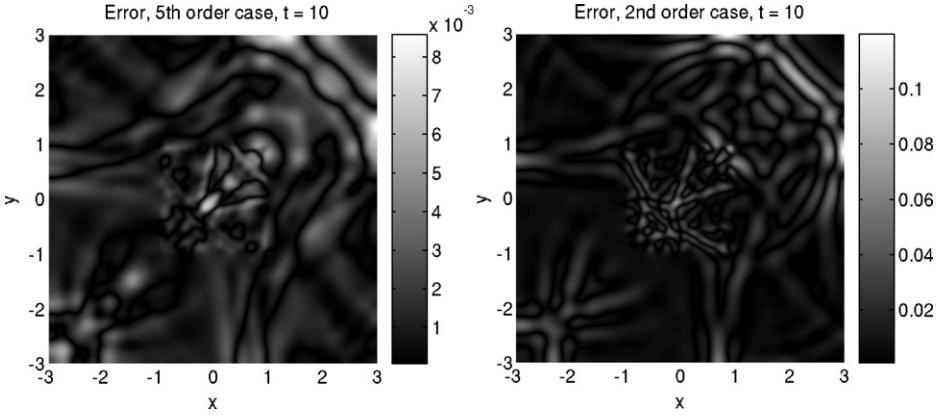

Fig. 7. The error at $t = 10$, comparing the 6th and 2nd order discretization.

As a last illustration we consider another problem on the 9-block domain. This time we initiate with planar waves going in the x-direction, see Fig. 8, where the solution at $t = 10$ is also shown. The solutions at $t = 1$ and $t = 3$ are shown in Fig. 9. The slowdown of the wave speed in the center block is clearly seen.

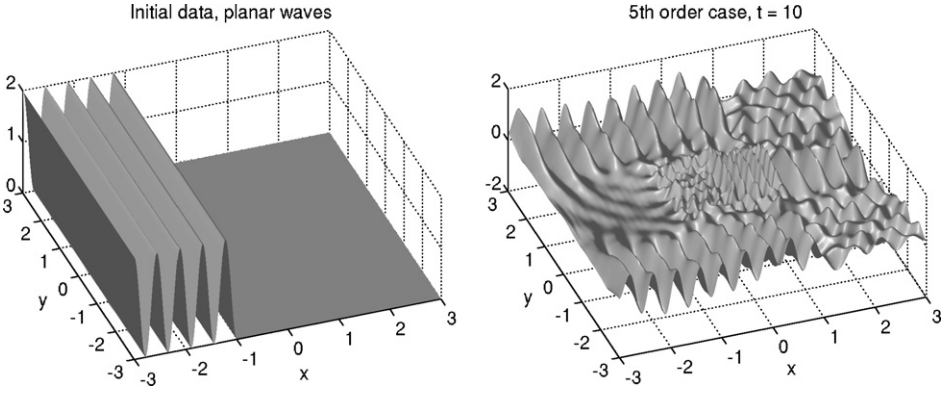

Fig. 8. Initial data, planar waves and the solution at $t = 10$. 6th order discretization. $N = (3 \times 97)^2$ unknowns.

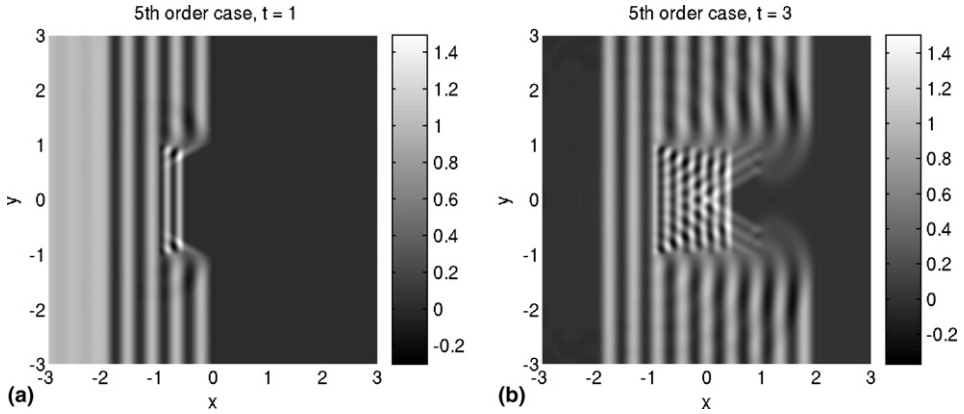

Fig. 9. Solution (initiated with planar waves) at $t = 1$ and $t = 3$. 6th order discretization and $N = (3 \times 97)^2$ unknowns. (a) $Re = 330$; (b) $Re = \infty$.

7. Conclusions and future work

Strictly stable and high order accurate finite difference schemes for the wave equation on second order form and discontinuous media are derived. A certain class of the recently developed compact second derivative SBP operators have been combined with the projection method for implementing boundary and interface conditions. We have shown that the projection method requires special treatment at corners and block interfaces in two dimensions to be well defined. The efficiency and high order accuracy of this method is verified by numerical simulations in one and two dimensions.

The methodology is so far restricted to rectangular geometries and piecewise constant coefficients. The extension to complex geometries and variable wave speeds can be done by using a hybrid technique like the one proposed in [9,10], where an unstructured finite volume method is combined (using the SAT method) with a high order finite difference method. This will be pursued in a coming paper.

Appendix I

Proof of Lemma 4.1. To investigate linear dependence we study

$$\sum_{j=1}^{N-1} \alpha_j (L_S)_j + \sum_{j=1}^{N-1} \beta_j (L_W)_j + \sum_{j=1}^{N-1} \sigma_j (L_N)_j + \sum_{j=1}^{N-1} \gamma_j (L_E)_j + \alpha L_{SW} + \beta L_{NW} + \sigma L_{NE} + \gamma L_{SE} = 0,$$

where we let $M = N$. This is equivalent to the following two systems of equations

$$\begin{aligned} &\frac{s_0}{h_x} \sum_{k=1}^{N-1} \beta_k e_k - \frac{s_0}{h_x} \sum_{k=1}^{N-1} \gamma_k e_k + \alpha \left(\frac{1-\eta_{SW}}{h_y} \sum_{k=0}^{N} s_k e_k + \frac{\eta_{SW}}{h_x} s_0 e_0 \right) + \beta \left(-\frac{1-\eta_{NW}}{h_y} \sum_{k=0}^{N} s_{N-k} e_k + \frac{\eta_{NW}}{h_x} s_0 e_N \right) \\ &\quad + \gamma \left(-\frac{1-\eta_{NE}}{h_y} \sum_{k=0}^{N} s_{N-k} e_k - \frac{\eta_{NE}}{h_x} s_0 e_N \right) + \sigma \left(\frac{1-\eta_{SE}}{h_y} \sum_{k=0}^{N} s_k e_k - \frac{\eta_{SE}}{h_x} s_0 e_0 \right) = 0 \end{aligned} \tag{45}$$

and

$$\begin{aligned} &\frac{s_j}{h_x} \sum_{k=1}^{N-1} \beta_k e_k - \frac{s_{N-j}}{h_x} \sum_{k=1}^{N-1} \gamma_k e_k + \frac{\alpha_j}{h_y} \sum_{k=0}^{N} s_k e_k - \frac{\sigma_j}{h_y} \sum_{k=0}^{N} s_{N-k} e_k + \alpha \eta_{SW} \frac{s_j}{h_x} e_0 \\ &\quad + \beta \eta_{NW} \frac{s_j}{h_x} e_N - \gamma \eta_{NE} \frac{s_{N-j}}{h_x} e_N - \sigma \eta_{SE} \frac{s_{N-j}}{h_x} e_0 = 0, \quad j = 1, \ldots N-1. \end{aligned} \tag{46}$$

The first component (that corresponds to $s_0 e_0$) in (45) leads to

$$\alpha(h_x(1-\eta_{SW}) + h_y \eta_{SW}) s_0 + \sigma(h_x(1-\eta_{SE}) - h_y \eta_{SE}) s_0 = 0$$

and there are only two non-trivial solutions

$$\text{(i)} \quad \eta_{SE} = \frac{h_x}{h_x + h_y}, \qquad \text{(ii)} \quad \alpha = \sigma \frac{h_x(1-\eta_{SE}) - h_y \eta_{SE}}{h_x(1-\eta_{SW}) + h_y \eta_{SW}},$$

since $0 \leqslant \eta_{SW}, \eta_{SE}, \leqslant 1$ and $s_0 \neq 0$ for any SBP operator. The second solution violates (46) and must be discarded. Hence, $\eta_{SE} \neq \frac{h_x}{h_x+h_y}$ implies $\alpha = \sigma = 0$. The last component (that corresponds to $s_0 e_N$) in (45) leads to

$$\beta(-h_x(1-\eta_{NW}) + h_y \eta_{NW}) s_0 - \gamma(h_x(1-\eta_{NE}) + h_y \eta_{NE}) s_0 = 0$$

and again there are only two non-trivial solutions

$$\text{(i)} \quad \eta_{NW} = \frac{h_x}{h_x + h_y}, \qquad \text{(ii)} \quad \gamma = -\beta \frac{h_x(1-\eta_{NW}) + h_y \eta_{NW}}{h_x(1-\eta_{NE}) + h_y \eta_{NE}},$$

and again only the first solution is valid. If $\eta_{NW} \neq \frac{h_x}{h_x+h_y}$ necessarily $\beta = \gamma = 0$. From the remaining components in (45) we then obtain β_j, $\gamma_j = 0$, $j = 1, \ldots, N-1$. This in turn, by utilizing (46), implies that α_j, $\sigma_j = 0$, $j = 1, \ldots, N-1$. The columns of L are thus linearly independent iff $\eta_{NW}\eta_{SE} \neq \frac{h_x}{h_x+h_y}$, i.e., L has full rank. □

Appendix II. Symmetric second derivative SBP operators

We now present the specific form of the symmetric SBP operators used in the analysis. We consider the 2nd and 6th order accurate discretizations.

Appendix II.1. Second order symmetric SBP operator

The discrete norm is given by $H = h\,\mathrm{diag}(\frac{1}{2}, 1, \ldots, 1, \frac{1}{2})$. The discrete second order accurate symmetric SBP operator $D_2 = H^{-1}(-A + BS)$ approximating $\frac{d^2}{dx^2}$ and the boundary derivative operator S are given by,

$$D_2 = \frac{1}{h^2}\begin{bmatrix} 1 & -2 & 1 & & \\ 1 & -2 & 1 & & \\ & \ddots & \ddots & \ddots & \\ & & 1 & -2 & 1 \\ & & 1 & -2 & 1 \end{bmatrix}, \quad S = \frac{1}{h}\begin{bmatrix} -\frac{3}{2} & 2 & -\frac{1}{2} & & \\ & 1 & & & \\ & & \ddots & & \\ & & & 1 & \\ & & \frac{1}{2} & -2 & \frac{3}{2} \end{bmatrix}.$$

Appendix II.2. Sixth order symmetric SBP operator

The discrete norm is given by $H = h\,\mathrm{diag}(\frac{13649}{43200}, \frac{12013}{8640}, \frac{2711}{4320}, \frac{5359}{4320}, \frac{7877}{8640}, \frac{43801}{43200}, 1, \ldots)$ and the discrete sixth order accurate symmetric SBP operator $D_2 = H^{-1}(-A + BS)$ approximating $\frac{d^2}{dx^2}$. The interior stencil is the standard sixth order accurate central scheme $h^2(D_2 v)_j = \frac{1}{90}v_{j-3} - \frac{3}{20}v_{j-2} + \frac{3}{2}v_{j-1} - \frac{49}{18}v_j + \frac{3}{2}v_{j+1} - \frac{3}{120}v_{j+2} + \frac{1}{90}v_{j+3}$. At the boundary the operator becomes:

$$D2 = \frac{1}{h^2}\begin{bmatrix} \frac{114170}{40947} & -\frac{438107}{54596} & \frac{336409}{40947} & -\frac{276997}{81894} & \frac{3747}{13649} & \frac{21035}{163788} & 0 & 0 & 0 & 0 \\ \frac{6173}{5860} & -\frac{2066}{879} & \frac{3283}{1758} & -\frac{303}{293} & \frac{2111}{3516} & -\frac{601}{4395} & 0 & 0 & 0 & 0 \\ -\frac{52391}{81330} & \frac{134603}{32532} & -\frac{21982}{2711} & \frac{112915}{16266} & -\frac{46969}{16266} & \frac{30409}{54220} & 0 & 0 & 0 & 0 \\ \frac{68603}{321540} & -\frac{12423}{10718} & \frac{112915}{32154} & -\frac{75934}{16077} & \frac{53369}{21436} & -\frac{54899}{160770} & \frac{48}{5359} & 0 & 0 & 0 \\ -\frac{7053}{39385} & \frac{86551}{94524} & -\frac{46969}{23631} & \frac{53369}{15754} & -\frac{87904}{23631} & \frac{820271}{472620} & -\frac{1296}{7877} & \frac{96}{7877} & 0 & 0 \\ \frac{21035}{525612} & -\frac{24641}{131403} & \frac{30409}{87602} & -\frac{54899}{131403} & \frac{820271}{525612} & -\frac{117600}{43801} & \frac{64800}{43801} & -\frac{6480}{43801} & \frac{480}{43801} & 0 \\ 0 & 0 & 0 & \frac{1}{90} & -\frac{3}{20} & 3/2 & -\frac{49}{18} & 3/2 & -\frac{3}{20} & \frac{1}{90} \\ & & & & & \ddots & \ddots & \ddots & \ddots & \end{bmatrix}$$

and the boundary derivative operator S of 4th order accuracy:

$$S = \frac{1}{h}\begin{bmatrix} -\frac{25}{12} & 4 & -3 & \frac{4}{3} & -\frac{1}{4} & & \\ & & 1 & & & & \\ & & & \ddots & & & \\ & & & & 1 & & \\ & & \frac{1}{4} & -\frac{4}{3} & 3 & -4 & \frac{25}{12} \end{bmatrix}.$$

References

[1] R. Glowinski, A. Bamberger, Q.H. Tran, A domain decomposition method for the acoustic wave equation with discontinuous coefficients and grid change, SIAM J. Num. Anal. 34 (2) (1997) 603–639.
[2] S. Abarbanel, A. Ditkowski, Asymptotically stable fourth-order accurate schemes for the diffusion equation on complex shapes, J. Comput. Phys. 133 (1997) 279–288.
[3] M.H. Carpenter, D. Gottlieb, S. Abarbanel, The stability of numerical boundary treatments for compact high-order finite-difference schemes, J. Comput. Phys. 108 (2) (1994).
[4] M.H. Carpenter, Jan Nordström, David Gottlieb, A stable and conservative interface treatment of arbitrary spatial accuracy, J. Comput. Phys. 148 (1999).
[5] G. Cohen, P. Joly, Construction and analysis of fourth-order finite difference schemes for the acoustic wave equation in nonhomogeneous media, SIAM J. Num. Anal. 33 (4) (1996) 1266–1302.
[6] A. Ditkowski, K. Dridi, J.S. Hesthaven, Convergent cartesian grid methods for Maxwell's equations in complex geometries, J. Comput. Phys. 170 (2001) 39–80.
[7] T.A. Driscoll, B. Fornberg, Block pseudospectral methods for Maxwell's equations II: two-dimensional, discontinuous-coefficient case, SIAM J. Sci. Comput. 21 (1999) 1146–1167.
[8] Gioel Calabrese et al., Summation by parts and dissipation for domains with excised regions, Classical Quantum Gravity 21 (2004) 5735–5757.
[9] J. Nordström, J. Gong, A stable and efficient hybrid method for aeroacoustic sound generation and propagation, Comptes Rendus Mecanique 333 (2005) 713–718.
[10] J. Nordström, J. Gong, A stable hybrid method for hyperbolic problems, J. Comput. Phys. 212 (2006) 436–453.
[11] B. Gustafsson, H.O. Kreiss, A. Sundström, Stability theory of difference approximations for mixed initial boundary value problems, Math. Comp. 26 (119) (1972).
[12] B. Gustafsson, E. Mossberg, Time compact high order difference methods for wave propagation, SIAM J. Sci. Comput. 26 (2004) 259–271.
[13] B. Gustafsson, P. Wahlund, Time compact difference methods for wave propagation in discontinuous media, SIAM J. Sci. Comput. 26 (2004) 272–293.
[14] T. Hagstrom, Radiation boundary conditions for the numerical simulations of waves, Acta Numerica 8 (1999) 47–106.
[15] H.-O. Kreiss, N.A. Petersson, J. Yström, Difference approximations for the second order wave equation, SIAM J. Num. Anal. 40 (2002) 1940–1967.
[16] H.-O. Kreiss, N.A. Petersson, J. Yström, Difference approximations of the Neumann problem for the second order wave equation, SIAM J. Num. Anal. 42 (2004) 1292–1323.
[17] H.-O. Kreiss, G. Scherer, Finite Element and Finite Difference Methods for Hyperbolic Partial Differential EquationsMathematical Aspects of Finite Elements in Partial Differential Equations, Academic Press, New York, 1974.
[18] H.-O. Kreiss, G. Scherer, On the existence of energy estimates for difference approximations for hyperbolic systems, Technical Report, Department of Scientific Computing, Uppsala University, 1977.
[19] L. Lehner, D. Neilsen, O. Reula, M. Tiglio, The discrete energy method in numerical relativity: towards long-term stability, Classical Quantum Gravity 21 (2004) 5819–5848.
[20] Ken Mattsson, Jan Nordström, Summation by parts operators for finite difference approximations of second derivatives, J. Comput. Phys. 199 (2) (2004).
[21] Jan Nordström, Mark H. Carpenter, Boundary and interface conditions for high order finite difference methods applied to the Euler and Navier–Stokes equations, J. Comput. Phys. 148 (1999).
[22] Jan Nordström, Mark H. Carpenter, High-order finite difference methods, multidimensional linear problems and curvilinear coordinates, J. Comput. Phys. 173 (2001).
[23] Pelle Olsson, Summation by parts, projections, and stability I, Math. Comp. 64 (1995) 1035.
[24] Pelle Olsson, Summation by parts, projections, and stability II, Math. Comp. 64 (1995) 1473.
[25] G.R. Shubin, J.B. Bell, A modified equation approach to constructing fourth order methods for acoustic wave propagation, SIAM J. Sci. Stat. Comput. 8 (2) (1987) 135–151.
[26] Bo Strand, Summation by parts for finite difference approximations for d/dx, J. Comput. Physics 110 (1994) 47–67.

[27] Bo Strand, High-order difference approximations for hyperbolic initial boundary value problems, Ph.D. Thesis, Uppsala University, Department of Scientific Computing, Uppsala University, Uppsala, Sweden, 1996.
[28] Magnus Svärd, Jan Nordström, On the order of accuracy for difference approximations of initial-boundary value problems, J. Comput. Phys. (2006) in press, doi:10.1016/j.jcp.2006.02.014.
[29] B. Szilagyl, H.-O. Kreiss, J.W. Winicour, Modeling the black hole excision problem, Physical Review D 71 (2005) 104035.
[30] S.V. Tsynkov, Numerical solution of problems on unbounded domains, a review, Appl. Num. Math. 27 (1998) 465–532.
[31] Z. Xie, C.H. Chan, B. Zang, An explicit fourth-order orthogonal curvilinear staggered-grid FDTD method for Maxwell's equations, J. Comput. Phys. 175 (2002) 739–763.